




Article

The Quaternary Climatic and Tectonic Development of the Murat River Valley (Muş Basin, Eastern Turkey) as Recorded by Fluvial Deposits Dated by Optically Stimulated Luminescence

Nurcan Avşin ^{1,*} , Mehmet Korhan Erturaç ^{2,3} , Eren Şahiner ⁴  and Tuncer Demir ⁵¹ Department of Geography, Van Yüzüncü Yıl University, Van 65000, Turkey² Department of Geography, Sakarya University, Sakarya 54050, Turkey; erturac@sakarya.edu.tr³ Research Development and Application Center (SARGEM), Esentepe Campus, Sakarya University, Sakarya 54187, Turkey⁴ Institute of Nuclear Sciences, Ankara University, Ankara 06560, Turkey; sahin@ankara.edu.tr⁵ Department of Geography, Akdeniz University, Antalya 07070, Turkey; tuncerdemir@akdeniz.edu.tr

* Correspondence: nurcanavsin@yyu.edu.tr or nurcanavsin@yahoo.com

Abstract: The paper describes climatic and tectonic effects on fluvial processes of East Anatolia. This study from the Muş Basin contains three alluvial terrace levels (T3-T1) ranging from 30–35 m to 3–5 m above the present Murat River in its middle section. In order to provide a chronology for the evaluation of the significant effects of climatic changes and tectonic uplift, we used optically stimulated luminescence (OSL) dating of the river deposits of the youngest (T3) and medium terrace (T2). The ages from these terrace deposits show that the T3 has formed approximately 6.5 ka ago, i.e., during the last part of the Holocene (MIS 1) and T2 has formed nearly 25 ka ago, i.e., during MIS 2 at the ending of the last glacial period. According to these results, it appears that the Murat River established its terrace sequences both in cold and warm periods. The variations in climate oriented fluvial evolution between the East Anatolia fluvial system and the temperate-periglacial fluvial systems in Europe may be the conclusion of different vegetation cover and melting thicker snow coverings in cold periods.

Keywords: river terrace; OSL dating; Murat River; Muş Basin; Turkey

Citation: Avşin, N.; Erturaç, M.K.; Şahiner, E.; Demir, T. The Quaternary Climatic and Tectonic Development of the Murat River Valley (Muş Basin, Eastern Turkey) as Recorded by Fluvial Deposits Dated by Optically Stimulated Luminescence. *Quaternary* **2021**, *4*, 29. <https://doi.org/10.3390/quat4030029>

Academic Editor: Pierre Antoine

Received: 1 July 2021

Accepted: 30 August 2021

Published: 14 September 2021

Publisher's Note: MDPI stays neutral with regard to jurisdictional claims in published maps and institutional affiliations.



Copyright: © 2021 by the authors. Licensee MDPI, Basel, Switzerland. This article is an open access article distributed under the terms and conditions of the Creative Commons Attribution (CC BY) license (<https://creativecommons.org/licenses/by/4.0/>).

1. Introduction

River terraces have been investigated for a long time from different regions of the world in order to restructure Quaternary climatic and tectonic conditions. This is because fluvial terraces are important archives which record the traces of the environmental changes during the Quaternary and before. They provide many morphological, stratigraphical, sedimentological and chronological data for reconstructing a specific landscape evolution. Generally, river terrace formation has been attributed to climatic variability and tectonic uplift [1–15]. Thus, especially in the formation of terrace sequences should be tectonic uplift in addition to the climatic effect [16–20].

The models which were revealed about the effects of climatic cycles on the valley evolution, focus on the stable and the unstable conditions which are linked to terrace forming process. For instance, Bridgland and Allen's model [2] implies that unstable climate transitions are relating terrace-forming incision, whereas Vandenberghe's model [21] suggested three scenarios of accumulation-erosion processes in climate-oriented terrace sequences accordingly the keeping chances of this development. According to these models, cold and warm periods are considered as relatively steady conditions. Towards the ending of glacial periods, river accumulation intensified especially in fields where glacier melt waters discharge together with sediment mass importantly rise [8,22].

A number of studies have presented a different setting for the deposition–incision stages in river valleys, referring accumulation to interglaciations [8,23–29]. For instance,

according to Stange et al. [8] the rivers terrace deposits accumulated in the marine isotope stages (MIS) 7 and 5 in the Pyrenees foreland and they reported that this fluvial activity occurred during the cold periods (stadials) within interglacials. In the West Carpathians terrace depositions appear to occur during MIS 5 and 3 which is expressed by the accumulation during the interstadials or interglacials comparable with the Holocene [27]. Schielein et al. [29] reported some terrace deposits from the northern Alpine foreland which reflects fluvial accumulation during both MIS 7 and 6, discerned by a clear border from each other.

A series of fluvial investigations in Turkey have aimed to clarify the timing of fluvial landscape evolution and its relationships with tectonics, inner dynamics and climatic changes. These studies displayed that a lot of rivers in Anatolia have been influenced by both climatic fluctuations and tectonic activities [18,23,25,30–37]. Avşın et al. [30] also found that fluvial aggradation in the Göksu River terraces in Southern Anatolia may have started in an interglacial period and keep gone in the next glacial phase. This result implies that some rivers may exhibit different behaviors from the mostly accepted fluvial response.

This paper aims to demonstrate the evolution of the terraces of the Murat River in East Anatolia using morphological analysis and OSL dating. We show that the fluvial development of the Murat River is dissimilar from those of temperate areas.

2. Physiography and Geological Framework

The study area is located in East Anatolia which is a region considerably affected by neotectonic deformations since the middle Miocene (Figure 1). More specifically, it is located near the junction of the NAF (North Anatolian Fault) and EAF (East Anatolian Fault). Thus, the Eastern Anatolian plateau represents the westernmost border of the biggest continental collision belt on Earth, stretching from the Turkish-Iranian-Caucasus orogen to the Himalayan-Tibetan orogen. This status arises from the collision of Arabia and India with Eurasia, together with the Central Anatolian plateau [38–40]. This process, which involves compressional tectonics, caused a large number of E-W extended basins especially in Eastern Anatolia. One of them is the Muş Basin, which is chosen as the present research area and has the character of an intermontane basin.

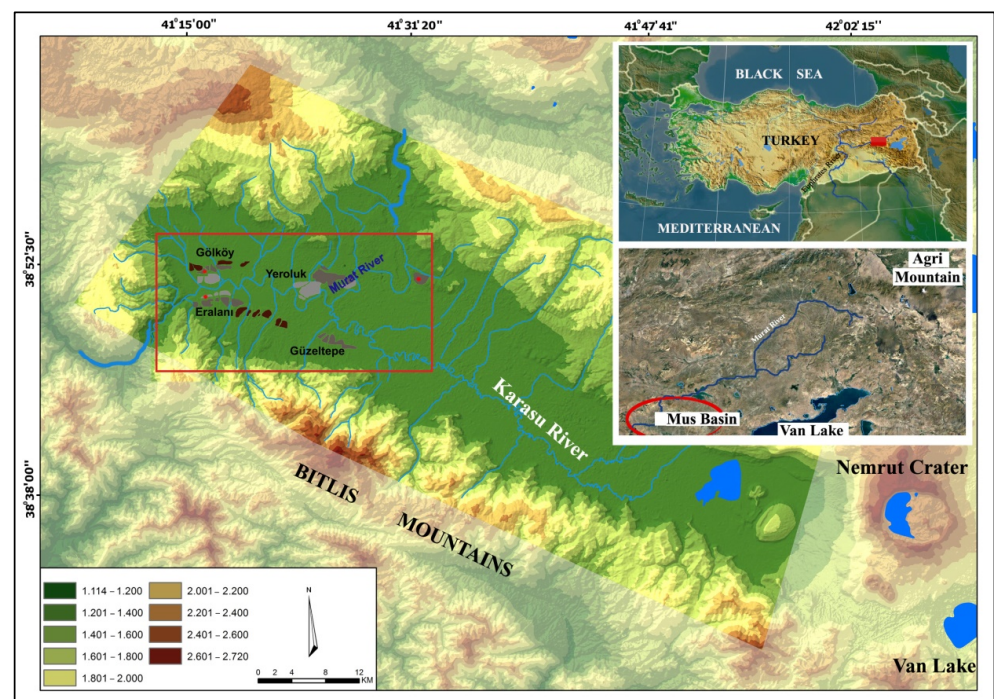


Figure 1. Location map of the study area.

The studied Murat River is the greatest tributary of the Euphrates River. It is mainly located within the Muş Basin, a tectonic depression in the East Anatolian plateau. The study area includes the middle section of the Murat River valley (Figure 1). In the latter area, the mean annual temperature is 9.5 °C, and the precipitation averaging 700 to 750 mm/year (General Directorate of Meteorology). The river has its headwaters near Ağrı Mountain and it has developed its course on mostly Pliocene lacustrine and Oligocene-Miocene terrestrial sediments. Thus, the Plio-Pleistocene lacustrine sediments and fan deposits are underlying the fluvial deposits. Previous morphological and geological studies reported that the basin has been affected by tectonism and this established the detailed course and fluvial characteristic of the Murat River [38,40–42].

3. Methods

3.1. Field Works and Sampling

The methods of this study comprise the traditional approaches as the determination of spatial and metric distribution of the river terraces by field observations, their geomorphological mapping, the sedimentary analyses of the terrace deposits, the sampling for OSL analysis and OSL dating. To restructure the paleo valley of the Murat River, the geomorphic map was made using 1:25,000 topographic and geological maps. The altitudes of terrace levels above the current riverbed were evaluated through the medium of a handheld GPS with error of 1 m. Terrace altitudes were measured at the base of the river deposits. The middle and the youngest terraces of the Murat River provide appropriate sand deposits for OSL dating, but the oldest terrace levels have not the required sand deposits. For the youngest terrace (T1) two samples from the same deposit and for the older terrace (T2) three samples from the separate deposits were collected for quartz OSL dating.

Sedimentary evaluations are mainly based on analyzing the concerned terrace exposures. Lithofacies identification and description were applied according to Miall's [43] sedimentary interpretations and internal properties, whereas the present-day river channel type was evaluated on the basis of Schumm's channel types [6,7] that is considered sinuosity-braiding degrees.

For understanding a possible influence of uplift and local tectonics on the development of the Murat River system, the possible faults were identified using not only conventional mapping, both also satellite images (such as Landsat). The uplift rate was calculated by the OSL ages of the terraces.

3.2. OSL (Optically Stimulated Luminescence) Dating

In this study Table 1 shows the used SAR-protocol, selecting preheat temperature at 220 °C, to avoid effect of unstable signals, which is suitable temperature for typical sedimentary quartz [44].

Table 1. Applied SAR protocol to samples.

Step	Treatment	Observed
1	Dose, D_i	
2	Preheat, 220 °C, 2 °C/s, 10 s	
3	OSL, 200 s at 125 °C, 2 °C/s	<i>Li</i>
4	Illumination, Blue 100 s	
5	Test dose, D_t	
6	Cutheat, 180 °C, 2 °C/s	
7	OSL, 200 s at 125 °C, 2 °C/s	<i>Ti</i>
8	Illumination, Blue 100 s at 280 °C	

At least 14–16 aliquots have been measured for each sample, obeying statistical approximation rules in radial distribution of EDs. Grains in the size range between 90–140 µm were selected and mounted on stainless steel discs as mono layer. The Central Age Model (CAM) was used towards assessing the corresponding ages. Figure 2a presents

a typical dose response curve for the corrected OSL signal, L_i/T_i of each sample, while Figure 2b presents the corresponding radial plot for selected sample, coded MUS-1A. The same protocol was applied for all samples in this framework.

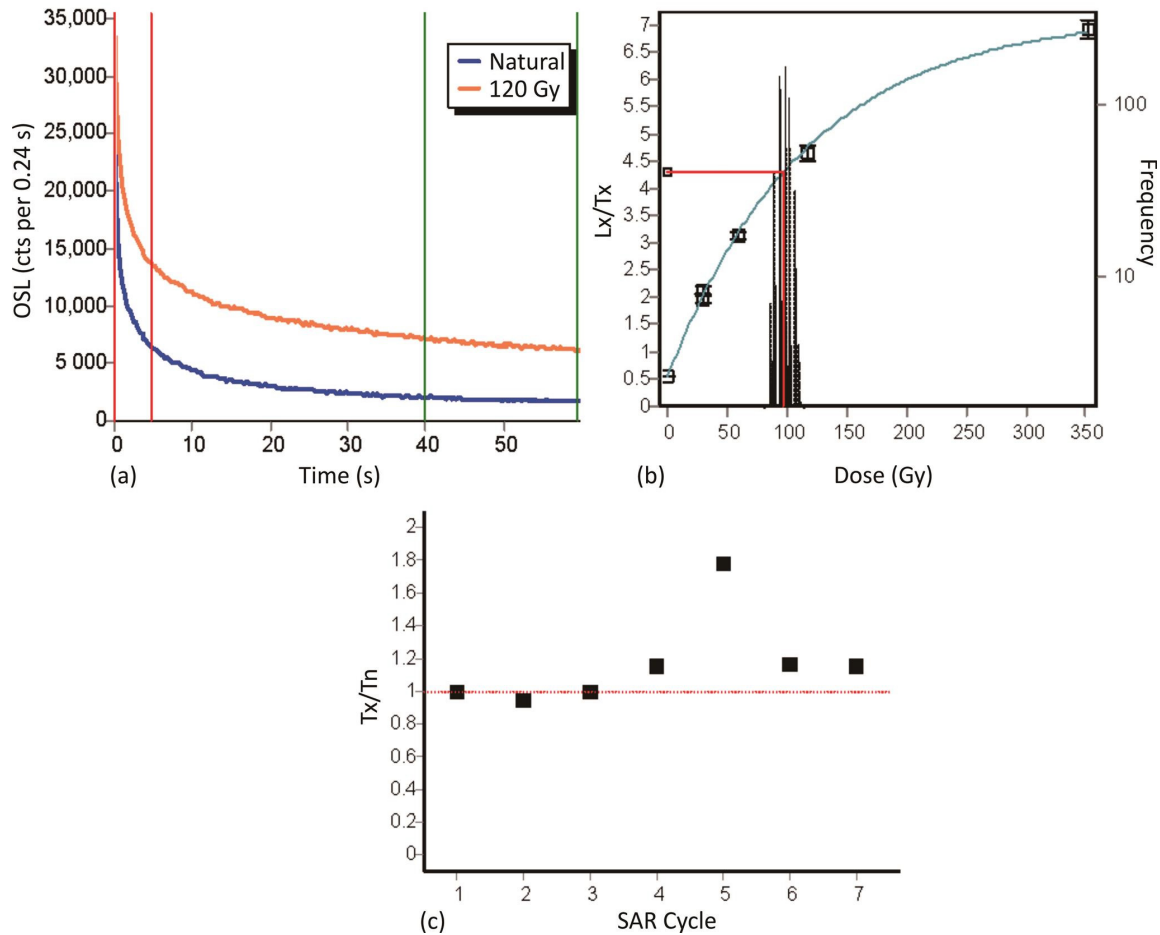


Figure 2. SAR analyses of the sample coded “MUS-1A” representing all samples. Exactly same analyses were performed for all samples (a) OSL shine-down of the sample for both natural and artificial doses. Initial 5 s used for integral and last 20 s for background (b) Dose response for the OSL signals of sample. The vertical left axes show the corrected OSL signal, the left axes Monte Carlo repeats of the calculated doses and the horizontal axes the laboratory radiation dose in Gy. The red dotted line also shows the ED. (c) Response to a testdose (T_x) normalized to the test dose response of the natural signal (T_n) throughout the measurements of sample showing the sensitivity changes occurring during the SAR-cycle.

The annual-dose rate is calculated based on the decay of naturally occurring radionuclides inside the sediment matrix, i.e., ^{232}Th and natural U-series and ^{40}K , together with cosmic rays. The concentrations of these elements are measured from samples extracted from each sample tube. Geochemical analyses were performed by an accredited geochemical laboratory (ALS-GLOBAL, İzmir, Turkey) using ICP-MS for trace elements (ALS Code: ME-MS81) and ICP-AES (ME-ICP06) for oxides. An outline of all the related data for the luminescence dating evolution is presented in Table 2. Environmental and cosmic dose rates (D_r) for each sample were calculated using the Dose Rate Calculator (DRC, Tsakalos et al., 2016) software (Table 2). Data outlined in Table 2 represents all the variables used in the determination of the OSL dates.

Table 2. Details of concentrations of the radioactive elements used for environmental dose rate estimations and age estimates for the samples.

Sample	U (ppm)	Th (ppm)	K (%)	Rb (ppm)	Terrace	LAT	LON	Z (m)	Depth (cm)	OD (%)	Disc	De CAM (Gray)	W (%)	Cosmic Dose Rate (Gray/ka)	Environmental Dose Rate (Gray/ka)	OSL AGE (ka)
OSL-1a	3.83 ± 0.19	13.05 ± 0.65	2.66 ± 0.13	91.3 ± 4.57	T2	38.85	41.25	1286	200	16	14	84.5 ± 3.7	29	0.14	3.52 ± 0.09	24.03 ± 1.21
OSL-1b	4.04 ± 0.2	14.95 ± 0.75	3 ± 0.15	113.5 ± 5.68	T2	38.85	41.25	1286	100	13	14	132.6 ± 6	27	0.17	4.01 ± 0.1	33.06 ± 1.72
OSL-4a	2.42 ± 0.12	8.68 ± 0.43	1.68 ± 0.08	70.7 ± 3.54	T1	38.84	41.3	1268	150	23	14	19.3 ± 1.4	32	0.15	2.25 ± 0.05	8.58 ± 0.66
OSL-4b	2.7 ± 0.14	9.5 ± 0.48	1.74 ± 0.09	74.3 ± 3.72	T1	38.84	41.3	1268	100	18	14	23.1 ± 1.1	28	0.17	2.49 ± 0.06	9.29 ± 0.5
OSL-5	1.6 ± 0.08	6.9 ± 0.35	1.2 ± 0.06	52.1 ± 2.61	T2	38.86	41.52	1295	200	17	16	37.8 ± 1.6	31	0.14	1.67 ± 0.04	22.7 ± 1.11

OSL measurements were performed with a Risø TL/OSL-DA-20 (Technical University of Denmark, Center for Nuclear Technologies, Roskilde, Denmark) reader equipped with a $^{90}\text{Sr}/^{90}\text{Y}$ beta particle source, delivering a nominal dose rate of 0.115 ± 0.004 Gy/s. A 9635QA photomultiplier tube was used for light detection. The stimulation wavelength is 470 (± 20) nm for the case of blue stimulation, delivering at the sample position a maximum power of 40 mW cm² the detection optics consisted of a 7.5 mm Hoya U-340 filter ($\lambda_p \sim 340$ nm, FWHM ~ 80 nm).

Laboratory preparation procedures and protocols include sieving in the dark room, followed by treatment with HCl (10%), H₂O₂ (35%) in order to remove calcites and organics, respectively. Subsequently, in order to separate quartz from bulk sediment, we used floating with heavy liquid using sodium polytung state (SPT). We adjusted the density to 2.62, 2.7 g/cm³ to separate feldspars and heavy minerals, respectively. Lastly, HF (40%, 45–60 min of handling) was used for etching the quartz crystal to eliminate alpha radiation and a final treatment with HCl (10%) to remove secondary carbonate, all in order to obtain a pristine quartz extract. Aliquots with mass of 2 mg each were prepared by mounting the material on stainless-steel disks. The signal quality of the extracted quartz minerals was controlled by “IR check”, it means by stimulating quartz grains with IRSL (at room temperature). The results proved there was no feldspar signal contribution tonquartz grains (except sample 5B, which has considerable IR intensity while compared with blue stimulation). Only for this sample, one more IR stimulation step at 50 °C 100 s is added between preheat and OSL stimulation steps in Table 1 in order to eliminate feldspar contribution in quartz luminescence emission. This additional optical method is commonly used to remove feldspar contribution in the quartz signal.

4. Results

4.1. Morphological and Sedimentological Description of the Terraces

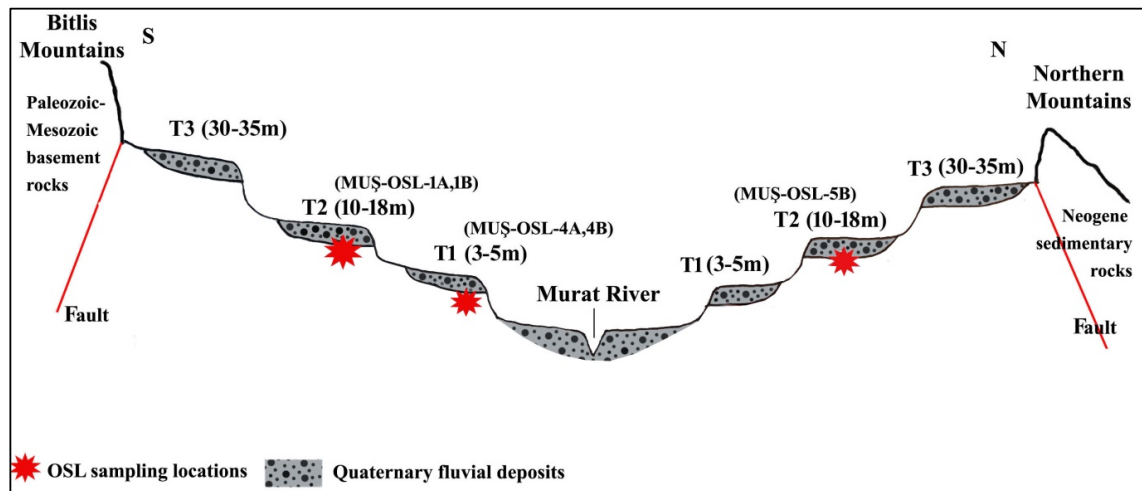
The Muş Basin, in which the Murat River is located, is drained by two river systems. One is the Murat River, which follows the basin in the N-S direction, while the other one is the Karasu River, which drains the basin in E-W direction and joins the Murat River in the west of the basin. Since the Karasu River does not form any terrace, only Murat River terraces are discussed in this study.

River terraces are present at three levels in the Murat River valley. They are distributed at heights of 3–5 m to 30–35 m above the present-day river level, and all terrace levels are identified at both sides of the river (Figure 3A, B). The terraces exhibit a stepped structure especially in the western part of the Muş Basin and at the Murat-Karasu river junction. The terrace elevations and longitudinal slopes decrease gradually in downward direction.

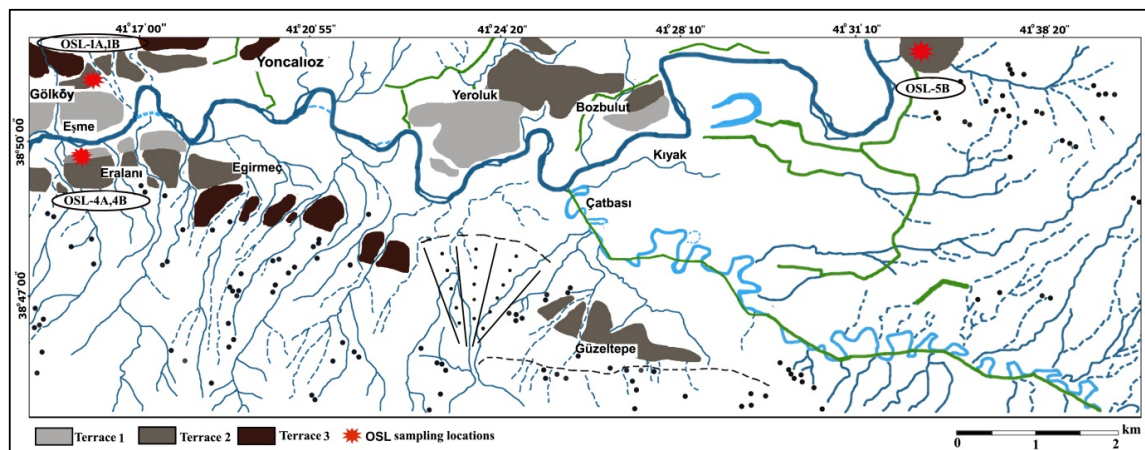
The terrace deposits in the research area consist of relatively well-preserved conglomerates with a thickness of 1–7.60 m. Even though there are some similarities between the sedimentological characteristics of the individual deposits, there are some remarkable differences in the grain size and stratification of these deposits. Alluvial fan and slope sediments are infrequently existing on top of the fluvial deposits

Terrace 3 (T3) is the highest terrace level in the field and appears at both sides of the river at a few locations, especially in the western part of the Muş Basin. This terrace level is generally covered with boulders to small pebbles (2–4 cm) without stratification.

Terrace 2 (T2) is the medium terrace in the area and it appears also at several locations and at both sides of the valley. In general, around Gök köy village, where two OSL samples (MUŞ-OSL-1A, 1B) were taken, and Güzeltepe village, the terrace deposits, with a thickness of 3–7.60 m, consist of well-cemented, crudely flatly bedded conglomerates (Gh) of coarse, matrix-supported, well to sub-rounded gravels, interbedded with fine sediments such as sand and clay.



(A)



(B)

Figure 3. (A) The generalized section of the Murat River valley and the OSL sampling locations. The elevations are basement levels of the fluvial terraces. (B) Stream terrace dispersion (the altitudes of T1, T2 and T3 are 30–35 m, 10–18 m, 3–5 m) in the middle section of the Murat River.

However, another fluvial deposit of the T2 level (around the Murat Bridge), from where the OSL sample MUŞ-OSL-5B has been taken, exhibits a different content consisting of clay, silt and sand layers. This content points to lower energy and discharge at this location. All deposits of T2 are much thicker than the deposits of other terraces and expose both clay, silt, sand and conglomerates in the outcrops around Gök köy and Murat Bridge.

Terrace 1 (T1) is the youngest terrace within the valley. This level especially occurs in the west of the basin at several locations such as around Eşme, Eralanı and Bozbulut villages. The deposits of T1 are composed of different sediments. For instance, around Bozbulut village, the internal structure of the 2–2.50 m thick deposit exhibits matrix-supported, loose, small pebbles. On the other hand, around Eşme the deposit with thickness of 3.80–4.00 m, consists of trough-shaped bedded sands and half rounded, clast-supported, coarse gravels (5–8 cm diameter) with interbedded clay and silt bands and horizontal layers of eroded

volcanic sediments. The deposit of T1 around Eralanı village where two OSL samples (MUŞ-OSL-4A, 4B) were taken, displays well-rounded, clast-supported, horizontally stratified, coarse gravels (10–15 cm diameter) and inclined stratified layers of clay, silt and sand.

4.2. OSL Dating Results

For luminescence dating of the terrace steps of the Murat River, five samples were picked up from three different places where available quartz bearing fine sand-silt layers are available (Figure 4). The sample localities are in the central and western part of the Muş Basin. T1 was sampled at Eralanı (38°50'17" N, 41°18'20" E) with samples OSL-4A and OSL-4B, whereas T2 is sampled from Gököy village (38°50'61" N, 41°15'07" E) (samples OSL-1A and OSL-1B) and around Murat Bridge (sample OSL-5B; (38°51'13" N, 41°26'79" E)).

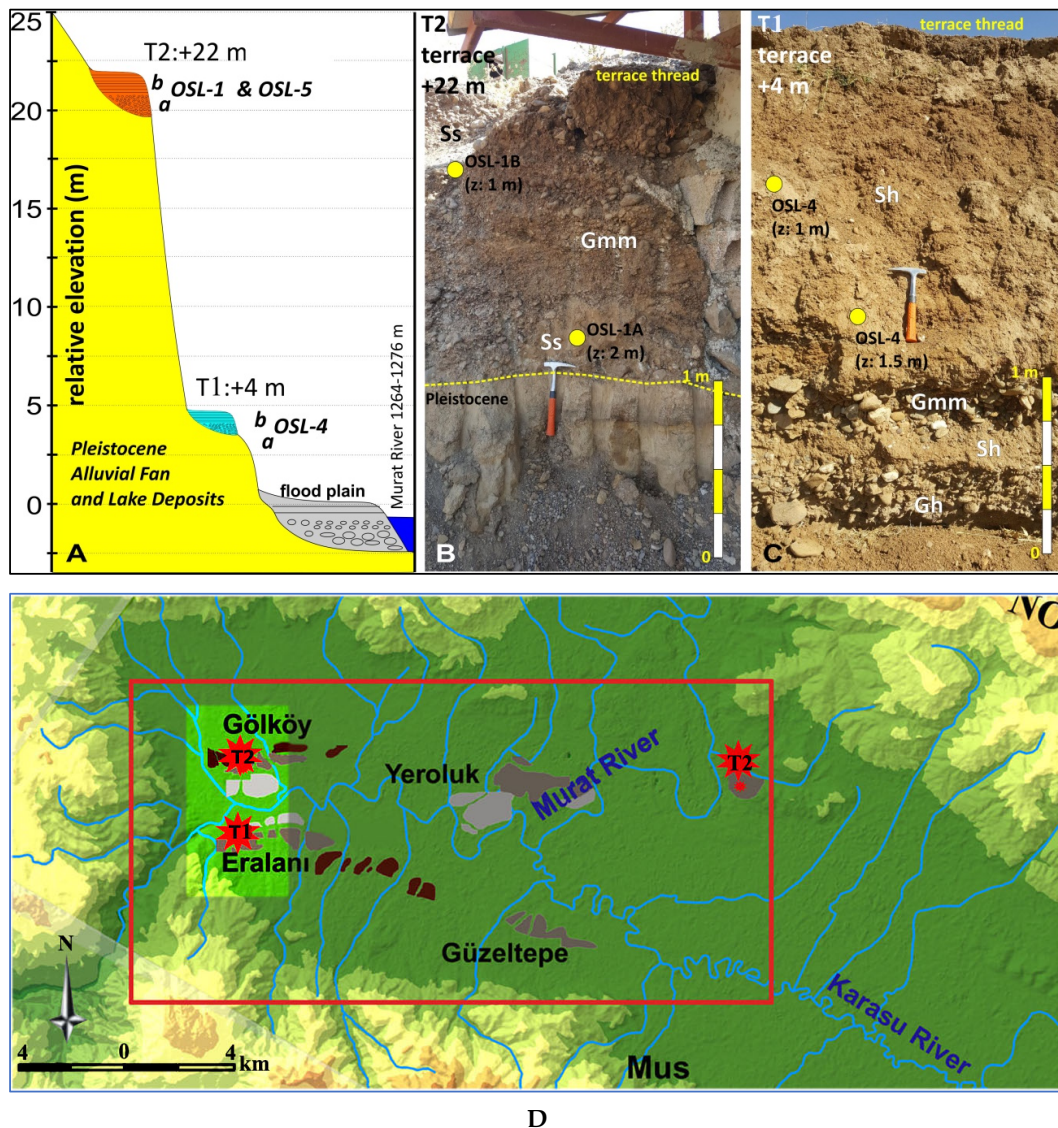


Figure 4. (A) Idealized cross-section of T1 and T2. (B) Sedimentological structure and OSL sampling location of T2 around Gököy village, displaying matrix-supported massive gravel ‘Gmm’, interbedded fine to coarse sand ‘Ss’. (C) Sedimentological record of T1 and OSL sampling location around Eralanı village, showing horizontal laminated sand ‘Sh’, matrix-supported, horizontal bedded gravels ‘Gh’ and matrix-supported massive gravel ‘Gmm’. (D) The locations of the T1 and T2 samples.

Table 2 A details the concentrations of the radioactive isotopes used to calculate the environmental dose rate (Dr) for each sample. It should be noted that the variations of each

element, which is reflected in D_r , changes from each focus section. This is strictly related to the basement lithology within the catchment of the tributaries of the Murat River. Mainly, clastics forming the Section 1 (OSL 1, T2) are derived from the northwest of the basin, where mafic Miocene-Pliocene volcanic and volcanoclastics are exposed. The sediments in Section 4 (OSL 4, T1) obtain clastics mostly from the Precambrian metamorphic rocks of the Bitlis Mountains in the south. Section 5 (OSL 5, T2) represents a larger catchment to the north of the Mus Basin with various types of bedrock lithologies such as Oligocene clastics and Miocene limestones.

Figure 5 represents the radial plots of equivalent dose (D_e) distribution for each dated sample. The overdispersion values (OD, Figure 5) from 14–16 aliquots are scattered between 13–23%, and all are acceptable for Central Age Model (CAM, Galbraith and Roberts, 2012) determination (Table 2).

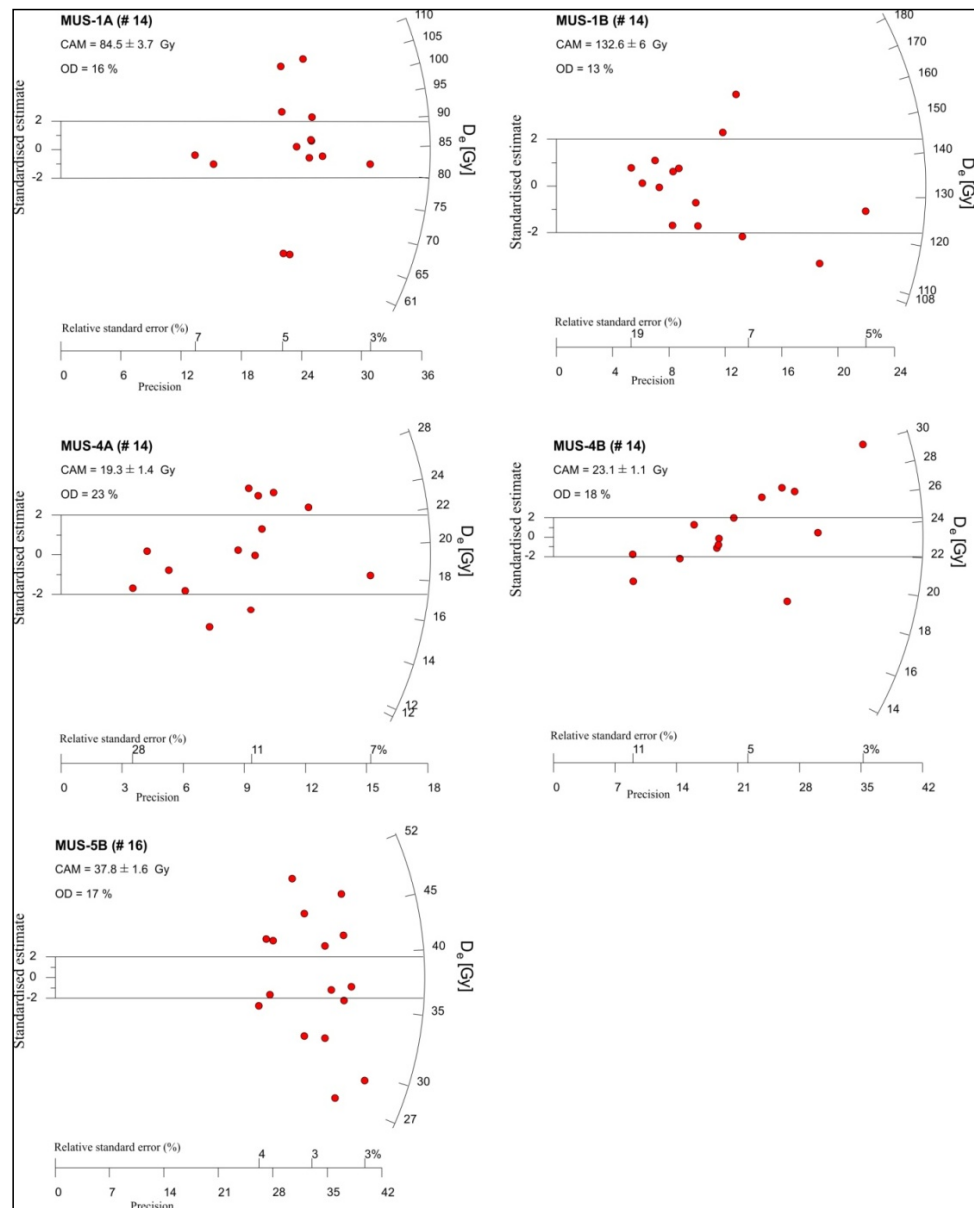


Figure 5. Radial distributions of EDs yielded (<2) after measuring 14–16 aliquots for each sample. The values with associated for individual aliquots are seen. The Central Age Model (CAM) was used in order to evaluate the corresponding ages.

According to the OSL ages, it may be derived that the two lower terrace steps of the Murat River had formed during two distinct periods. According to the age of OSL-1a and OSL-5, the older terrace T2 formed during the Last Glacial Maximum (LGM, MIS 2). The youngest terrace deposit (T1) dates from the end of the early Holocene (OSL-4), thus the MIS 1 interglacial period. The determined age of the OSL-1b sample is much older (10 ka) than OSL-1a and OSL-5 samples, although all of them were from T2. It exceeds the probable depositional period for the terrace. This age is considered an outlier, as the other two samples belonging to the T2 terrace level are outside the age, and perhaps due to insufficient bleaching.

5. Discussion

5.1. Tectonic Framework for the Valley Evolution

Reverse faults delineate the northern and southern borders of the Mus Basin. According to Şaroğlu and Güner [42], there was N-S contraction and crust thickening in Eastern Anatolia (Figure 6). This process caused the E-W stretched folds and thrusts (Bitlis Mountains), N-S directional opening cracks while the important river systems (as the Murat River) that form the valleys by perpendicular to the E-W stretching structures and the intermountain basins (Muş Basin sample).

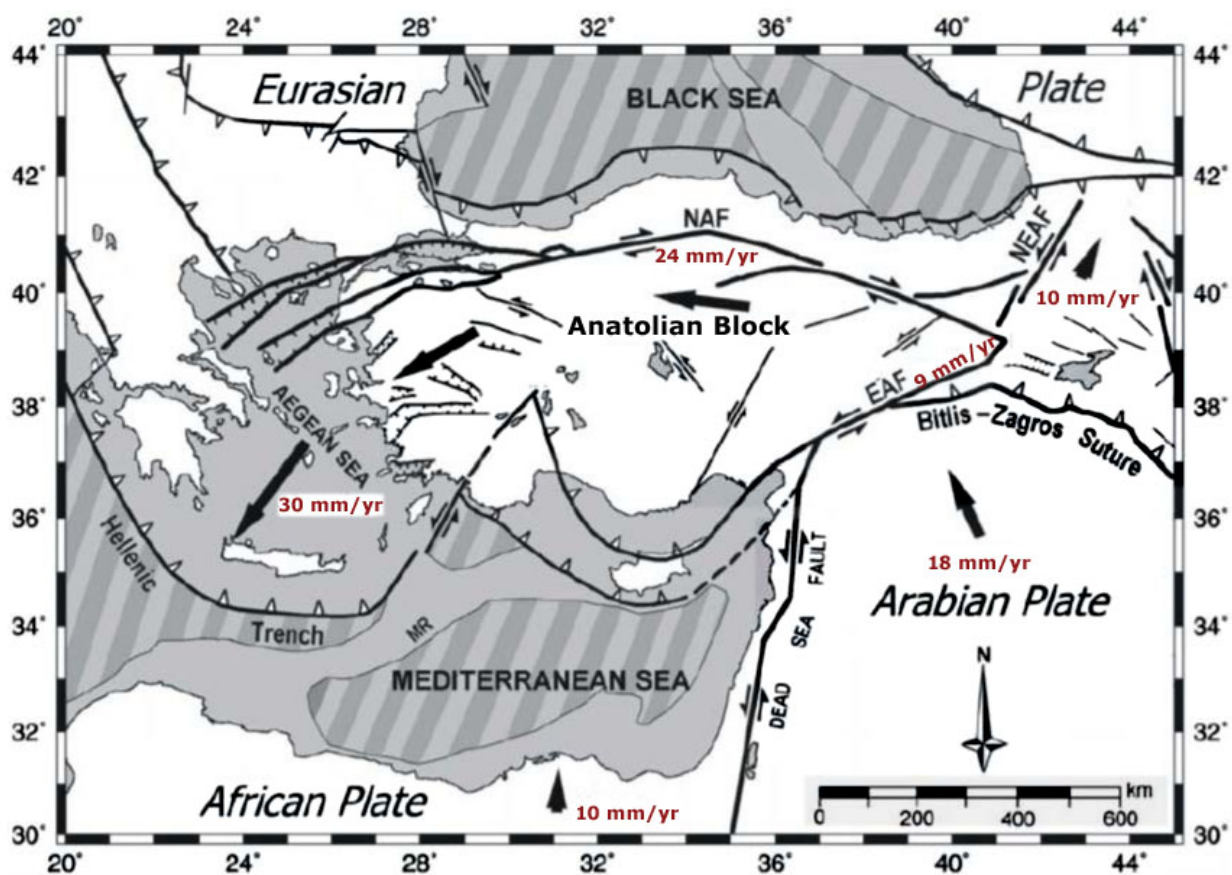


Figure 6. The simplified tectonic map of Turkey [45].

The Murat River, flowing in N-S direction from the northern Mountains towards the Basin, represents a powerful and erosive system resulting from the regional tectonic regime. In contrast, the Karasu River that is located in the same basin, flows in E-W direction which is parallel to and in the center of the Basin. It has a low longitudinal gradient (0.8 ‰) in contrast to the steep gradient (2.6 ‰) of the Murat River. The present-day pattern of the Karasu River is typically meandering with dominant accumulation (Figure 1).

In addition to these tectonic effects on river flow direction, gradients and pattern, there is the tectonic tilting in the Muş basin. According to drilling data (by The State Waterworks), in the east of the basin the Cenozoic sedimentary fill has a thickness of 450–500 m and in the west, the fills have a thickness of 200–250 m. Thus, it can be accepted that there is a general subsidence during the Cenozoic in the all basin and continuing subsidence in the east with uplift in the west during the Late Pleistocene. As a result of this tectonic process, the Karasu River displays a relatively wandering meandering channel pattern and doesn't have terraces, but the Murat River has a terrace sequence.

According to the OSL ages of the terraces, the fluvial incision rate is c. 0.4 mm/year for the last 8500 years for the youngest terrace. Similarly, it is 0.6 mm/year for the last 26,000 years for the middle terrace in the Muş Basin. It is important that this ratio offers an idea of the tectonic uplift on condition that the rivers obtained a (quasi-) equilibrium gradient at the time of terrace formation. In studies conducted in different rivers in Anatolia, various uplift rates have been reported depending on the age of terrace deposits. For example, the uplift rate determined for the Göksu River valley in southern Anatolia is 0.05 mm/yr. For the Seyhan River valley, which is another southern Anatolian river, this ratio is 0.11 mm/yr. On the other hand, while this ratio is between 0.042–0.12 mm/yr for the Kızılırmak River valley in Central Anatolia, it is 0.15 mm/yr for the Euphrates River valley in the Southeast Anatolian region. The Muş Basin proves the high tectonic activity of the Eastern Anatolia region with its relatively high uplift rate.

However, some local faults are present, especially in the mountains (Otluk and Bitlis Mountains) north and south of the Muş Basin. However, we couldn't determine the direct effects of these faults at the terrace levels as a tilting throughout the longitudinal profiles.

5.2. Sedimentary Interpretation of the Terrace Deposits and Reconstruction of the Paleo-River Valley

The present-day Murat River is low sinuosity and has point bars or chute cutoff bars (Figure 7). The sinuosity is calculated as 1.3 and this value implies a wandering river type [43] which is supported by the mostly interbedded coarse-grained and fine-grained sediments. According to these properties of the terrace deposits, the older Murat River also had a similar channel type, both during the interglacial periods (the Holocene terrace, T1) and the cold periods (the Pleistocene terrace, T2).



Figure 7. The present-day Murat River.

Moreover, each terrace level of the Murat River has relatively similar sedimentary structure and facies succession. In the deposit of T3, the youngest terrace, well-rounded, clast-supported, horizontally stratified coarse gravels and inclined stratified layers of clay, silt and sand are dominant. Thereby, this facies is valuated as representing a mixed-load, wandering channel [43].

The middle terrace (T2) displays well-cemented, crude flatly bedded conglomerates (Gh) with coarse, matrix-supported well or sub-rounded gravels, interbedded with fine sediments such as sand and clay. In this case, during the formation of T2, the river was wandering and had a variable fluvial energy, but during the next phase (when the forming of T1) this wandering river still occurred and had a lower energy condition. We suggest that, when the river begun to accumulate in MIS 2 (MUŞ-OSL-1A, 1B), it was relatively energetic. In the later stage of the river aggradation (MIS 1—MUŞ-OSL-4A, 4B), the energy reduced and the river begun to aggrade relatively fine-grained sediments (Figure 8).

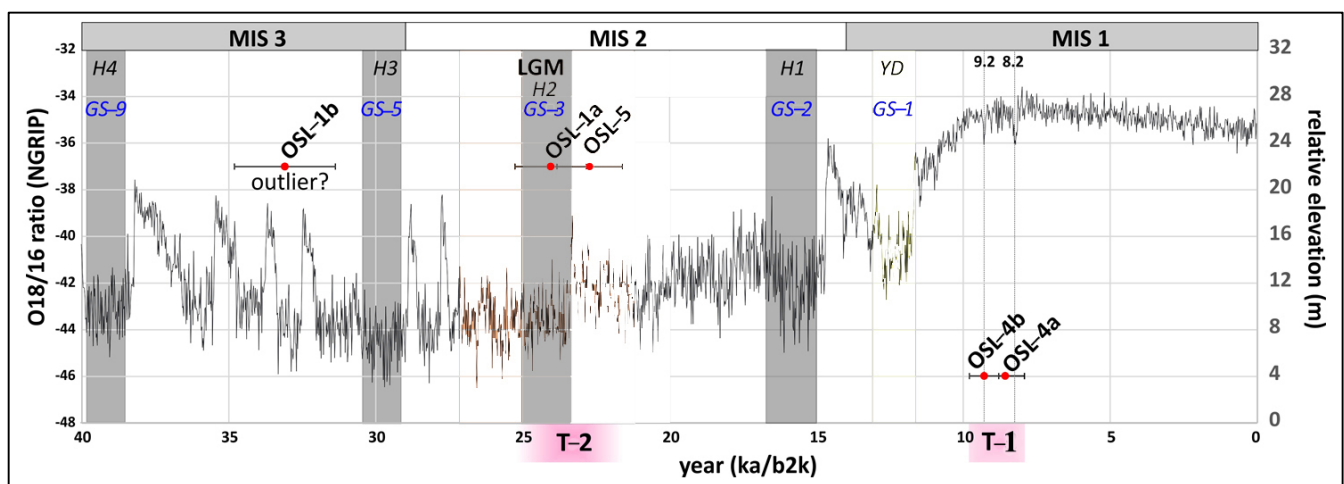


Figure 8. Correlation of OSL ages from two steps in the terrace staircase of the Muş Basin with NGRIP ice core d18O data (NGRIP Members, 2014), (MIS boundaries from Lisiecki and Raymo, 2005) and (Heinrich events and Greenland Stadials, according to Rasmussen et al., 2014). T2 has been deposited during the LGM and coincides with the H2 cold period. T3 marks the end of the early Holocene.

5.3. Climatic Impact

In the investigated valley, we evaluated the ages of T2 and T1 since T3, which is the oldest terrace of the Murat River could not be dated due to the absence of suitable sediments for dating. It is a reasonable hypothesis that considering that the T1 was formed at the MIS 1 Holocene interglacial period and the T2 was formed at the MIS 2 glacial period, T3 may have created at the MIS 3 interstadial time (Figure 8). Therefore, the age of T3 should be in the range of 35–60 ka.

The deposits of T2 during the last glacial period (MIS 2) around Gököy village where two OSL dating samples were taken, and around Güzeltepe village have a mixed-load sediment with the horizontal bedded gravel and sand layers, while another deposit of the same terrace around the Murat Bridge, where the OSL dating sample was taken, consists of fine sediments (fine-grained sand, clay and silt beds). Thus, it is possible that the Murat River had changed its energy in the glacial period.

The facies of the interglacial period (MIS 1, the age of 8.5 ka) around Eralanı village where two OSL dating samples were taken in the west boundary of the Muş Basin, are composed of relatively finer sediment and it also display interbedded mixed-load sediments with medium to fine gravel and sand beds.

Therefore it seems that climatic conditions in the region have controlled and shaped the internal structure of the terraces. According to the features of T2 deposits, in the cold periods both relatively coarse-grained sediment and fine-grained sediment accumulation

has occurred in Murat River valley. In the warm periods (according to the internal features of T1) finer sediment has aggradated due to declining the river energy. However, in the transition periods (cold to warm, warm to cold) the river had fluvial incision. Especially in the period of cold to warm transition the snow melting had affected the river energy a lot. Otherwise, the changes of vegetation cover at the beginning of climatic warming was important.

The balance, which between discharge (transport capacity) and sediment load of the river, results from different factors, as climate and vegetation cover. Accepting the rain steady, because of no information we have, an approach is taken to clarify the differences in fluvial evolution between the Mediterranean environment and the cool temperate environment as we did for the nearby Goksu valley [30]. According to Vandenberghe [12,46,47], the vegetation cover is so effective in managing sediment deposit in to valleys. Reduced sediment supplies due to delayed response of vegetation growth or decreasing with respect to climate effect induce river incision during climatic transitions in temperate terms [12]. Some studies show that this process was different in Anatolia. For instance, the exhaustive analyses of the Van Lake pollen show that xerophytic steppe vegetation was dense in Eastern Anatolia during MIS 2 and there were quick enlargements and contractions of tree populations that display changeability in temperature and moisture conditions [48]. Similarly, Messager et al. [49] revealed from pollen analyses of sediment cores in Lake Paravani (Georgia) that there were steppes in this region during cold periods. Şenkul and Doğan [50] also reported that the vegetation cover occupied 80–90% of the Northwestern Turkey and the Black Sea seaside, and 50–60% throughout the Mediterranean seaside during the last glacial period.

Thus, it is inferred that Anatolia had a steppic vegetation cover in the cold periods because of the less severe glacial climate than in other regions with colder environments. Therefore, sedimentary activities and channel patterns during glacial periods were probably so similar to those during interglacial periods. This small changes of vegetation in analogy with cooler temperate areas and the absence of temporary or permanent frozen land would have blocked an erosional impact at the warm-cold transition [30]. According to this, we can say that the local conditions such as as vegetation cover, may significantly influence fluvial evolution. Even though it is difficult to comment based on the OSL analysis of the not many samples, the climate driven fluvial process that is displayed by the analysis, supports the other study results in Anatolia. Thus, it can be said that there is a little different climate-fluvial system relationship in Anatolia in the presence of partial data that is compatible with other studies.

6. Conclusions

In the Murat River valley, located in the Muş Basin, East Anatolia (warm continental middle latitudes), the development of fluvial terraces is closely related to climatic cycles and driven by tectonic uplift. Based on the results of the OSL dating of T2 and T1, it can be said that the Murat River aggravated its facieses under varied climatic conditions. T2 was deposited during the MIS 2 cold period, whereas T1 was deposited during the Holocene interglacial (MIS 1). Thus, the river begun to aggrade in MIS 2 and was relatively energetic. In the next stage of the river aggradation, the energy reduced and the river begun to deposit relatively fine sediments. Based on the OSL ages, it is remarkable that the stream channel pattern (wandering type) and sedimentologic features (terrace 2 and 3) between glacial and interglacial times were not so different and that river erosion was not distinct at the warm-to-cold transition. The river incision at the cold-to-warm transition was caused by the impact of the snow melting rather than the changes of vegetation cover at the inception of climatic warming. As a result, it may be verified from this study that local situations may substantially affect fluvial evolution.

Author Contributions: Conceptualization, N.A. and M.K.E.; methodology, E.Ş. and M.K.E.; software, N.A., M.K.E., E.Ş. and T.D.; validation, N.A., M.K.E. and E.Ş.; formal analysis, E.Ş.; investigation, N.A.; resources, N.A., T.D.; data curation, N.A., M.K.E.; writing—original draft preparation, N.A., M.K.E., E.Ş.; writing—review and editing, N.A., T.D.; visualization, N.A., M.K.E., E.Ş.; supervision,

T.D.; project administration, N.A.; funding acquisition: N.A. All authors have read and agreed to the published version of the manuscript.

Funding: This research received no external funding.

Institutional Review Board Statement: Not applicable.

Informed Consent Statement: Not applicable.

Acknowledgments: This study is financially supported by Yüzüncü Yıl University—Scientific Research Projects (2016-SOB-Author Contributions: D043). In addition, we like to thank İsmail Kader who helped with our security in the field and to thank Ahmet Turan who contributed to the field studies and the sampling of the terrace deposits. In addition, we would like to thank Jef Vandenberghe for contributing to the improvement of this study.

Conflicts of Interest: The authors declare no conflict of interest.

References

1. Antoine, P.; Lautridou, J.P.; Laurent, M. Long-Term Fluvial archives in NW France: Response of the Seine and Somme Rivers to Tectonic movements, Climatic variations and Sea level changes. *Geomorphology* **2000**, *33*, 183–207. [[CrossRef](#)]
2. Bridgland, D.; Allen, P. A revised model for terrace formation and its significance for the lower Middle Pleistocene Thames terrace aggradations of northeast Essex, UK. In *The Early Middle Pleistocene in Europe*; Turner, C., Ed.; Balkema: Rotterdam, The Netherlands, 1996; pp. 121–134.
3. Bridgland, D. River terrace systems in northwest Europe: An archive of environmental change, uplift and early human occupation. *Quat. Sci. Rev.* **2000**, *19*, 1293–1303. [[CrossRef](#)]
4. Maddy, D. Uplift-driven valley incision and river terrace formation in Southern England. *J. Quat. Sci.* **1997**, *12*, 539–545. [[CrossRef](#)]
5. Mol, J.; Vandenberghe, J.; Kasse, C. River response to variations of periglacial climate. *Geomorphology* **2000**, *33*, 131–148. [[CrossRef](#)]
6. Schumm, S. *The Fluvial System*; The Blackburn Press: Blackburn, UK, 1977.
7. Schumm, S. *Evolution and Response of the Fluvial System: Sedimentologic Implications*, Society of Economic Paleontologists and Mineralogists; Spec. Publ: The American Association Petroleum Geologist, OK, USA, 1981; Volume 31, pp. 19–29.
8. Stange, K.; Van Balen, R.T.; Carcaillet, J.; Vandenberghe, J. Terrace staircase development in the Southern Pyrenees Foreland: Inferences from ¹⁰Be terrace exposure ages at the Segre River. *Glob. Planet. Chang.* **2013**, *101*, 97–112. [[CrossRef](#)]
9. Starkel, L. Climatically terraces in uplifting mountain areas. *Quat. Sci. Rev.* **2003**, *22*, 2189–2198. [[CrossRef](#)]
10. Starkel, L.; Michczynska, D.; Gebica, P.; Kiss, T.; Panin, A. Climatic fluctuations reflected in the evolution of fluvial systems of Central-Eastern Europe (60–8 ka cal BP). *Quat. Int.* **2015**, *388*, 97–118. [[CrossRef](#)]
11. Tebbens, L.; Veldkamp, A. Exploring the possibilities and limitations of modelling Quaternary fluvial dynamics. In *River Basin Sediment Systems: Archives of Environmental Change*; Maddy, D., Macklin, M., Woodward, J., Eds.; Balkema: Rotterdam, The Netherlands, 2001; Chapter 17; pp. 469–484.
12. Vandenberghe, J. Timescales, climate and river development. *Quatern. Sci. Rev.* **1995**, *14*, 631–638. [[CrossRef](#)]
13. Vandenberghe, J.; Maddy, D. Response of river systems to climate change. *Quat. Int.* **2002**, *79*, 1–3. [[CrossRef](#)]
14. Vandenberghe, J.; Wang, X.; Lu, H. Differential impact of small-scaled tectonic movements on fluvial morphology and sedimentology (the Huang shui catchment, NE Tibet Plateau). *Geomorphology* **2001**, *134*, 171–185. [[CrossRef](#)]
15. Wang, X.; Vandenberghe, J.; Shuangwen, Y.; Van Balen, R.T.; Lu, H. Climate-dependent fluvial architecture and processes on a suborbital timescale in areas of rapid tectonic uplift: An example from the NE Tibetan Plateau. *Glob. Planet. Chang.* **2015**, *133*, 318–329. [[CrossRef](#)]
16. Bridgland, D.; Westaway, R. Climatically controlled river terrace staircases: A worldwide Quaternary phenomenon. *Geomorphology* **2008**, *98*, 285–315. [[CrossRef](#)]
17. Gibbard, P.L.; Lewin, J. River incision and terrace formation in the Late Cenozoic of Europe. *Tectonophysics* **2009**, *474*, 41–55. [[CrossRef](#)]
18. Maddy, D.; Demir, T.; Bridgland, D.; Veldkamp, A.; Stemerink, C.; van der Schriek, T.; Westaway, R. An obliquity controlled Early Pleistocene river terrace record from Western Turkey. *Quat. Res.* **2005**, *63*, 339–346. [[CrossRef](#)]
19. Peters, G.; Van Balen, R.T. Pleistocene tectonics inferred from the fluvial terraces of the northern Upper Rhine Graben, Germany. *Tectonophysics* **2007**, *430*, 41–65. [[CrossRef](#)]
20. Vandenberghe, J. The fluvial cycle at cold-warm-cold transitions in lowland regions: A refinement of theory. *Geomorphology* **2008**, *98*, 275–284. [[CrossRef](#)]
21. Vandenberghe, J. River terraces as a response to climatic forcing: Formation processes, sedimentary characteristics and sites for human occupation. *Quat. Int.* **2015**, *370*, 3–11. [[CrossRef](#)]
22. Cordier, T.; Robin, C.; Capdevielle, X.; Fabreguettes, O.; Desprez-Loustau, M.; Vacher, C. The composition of phyllosphere fungal assemblages of European beech (*Fagus sylvatica*) varies significantly along an elevation gradient. *New Phytol.* **2012**, *196*, 510–519. [[CrossRef](#)]

23. Avşın, N.; Vandenberghe, J.; van Balen, R.; Kıyak, N.; Öztürk, T. Tectonic and climatic controls on Quaternary fluvial processes and river terrace formation in a Mediterranean setting, the Göksu River, southern Turkey. *Quat. Res.* **2019**, *91*, 533–547. [[CrossRef](#)]
24. Camacho, M.E.; Quesada-Román, A.; Mata, R.; Alvarado, A. Soil-geomorphology relationships of alluvial fans in Costa Rica. *Geoderma Regional* **2020**, *21*, e00258. [[CrossRef](#)]
25. Dogan, U. Climate-controlled river terrace formation in the Kızılırmak Valley, Cappadocia section, Turkey: Inferred from Ar–Ar dating of Quaternary basalts and terraces stratigraphy. *Geomorphology* **2011**, *126*, 66–81. [[CrossRef](#)]
26. Olszak, J. Evolution of fluvial terraces in response to climate change and tectonic uplift during the Pleistocene: Evidence from Kamienica and Ochotnica River valleys (Polish Outer Carpathians). *Geomorphology* **2011**, *129*, 71–78. [[CrossRef](#)]
27. Olszak, J.; Adamiec, G. OSL-based chronostratigraphy of river terraces in mountainous areas, Dunajec basin, West Carpathians: A revision of the climatostratigraphical approach. *Boreas* **2016**, *45*, 483–493. [[CrossRef](#)]
28. Quesada-Román, A.; Zamorano-Orozco, J.J. Geomorphology of the Upper General River Basin, Costa Rica. *J. Maps* **2019**, *15*, 95–101. [[CrossRef](#)]
29. Schielein, P.; Schellmann, G.; Lomax, J.; Preusser, F.; Fiebig, M. Chronostratigraphy of the Hochterassen in the lower Lech valley (North Alpine Foreland). *Quat. Sci. J.* **2015**, *64*, 15–29.
30. Avşın, N. The role of the climate and tectonics on the evolution of the Kızılırmak River terraces. *J. Geogr. Sci.* **2011**, *9*, 221–238.
31. Bridgland, D.; Demir, T.; Seyrek, A.; Daoud, M.; Abou Romieh, M.; Westaway, R. River terrace development in the NE Mediterranean region (Syria and Turkey): Patterns in relation to crustal type. *Quat. Sci. Rev.* **2017**, *166*, 307–323. [[CrossRef](#)]
32. Demir, T.; Yeşilnacar, İ.; Westaway, R. River terrace sequences in Turkey: Sources of evidence for lateral variations in regional uplift. *Proc. Geol. Assoc.* **2004**, *115*, 289–311. [[CrossRef](#)]
33. Demir, T.; Seyrek, A.; Westaway, R.; Guillou, H.; Scaillet, S.; Beck, A.; Bridgland, D. Late Cenozoic regional uplift and localised crustal deformation within the northern Arabian Platform in southeast Turkey: Investigation of the Euphrates terrace staircase using multidisciplinary techniques. *Geomorphology* **2012**, *165*, 7–24. [[CrossRef](#)]
34. Dogan, U. Fluvial response to climate change during and after the Last Glacial Maximum in Central Anatolia, Turkey. *Quat. Int.* **2010**, *222*, 221–229. [[CrossRef](#)]
35. Maddy, D.; Demir, T.; Bridgland, D.; Veldkamp, A.; Stemerink, C.; van der Schriek, T.; Schreve, D. The Pliocene initiation and Early Pleistocene volcanic disruption of the paleo-Gediz fluvial system, Western Turkey. *Quat. Sci. Rev.* **2008**, *26*, 2864–2882. [[CrossRef](#)]
36. Westaway, R.; Pringle, M.; Yurtmen, S.; Demir, T.; Bridgland, D.; Rowbotham, G.; Maddy, D. Pliocene and Quaternary regional uplift in western Turkey: The Gediz River terrace staircase and the volcanism at Kula. *Tectonophysics* **2004**, *391*, 121–169. [[CrossRef](#)]
37. Westaway, R.; Guillou, H.; Yurtmen, S.; Beck, A.; Bridgland, D.; Demir, T.; Scaillet, S.; Rowbotham, G. Late Cenozoic uplift of western Turkey: Improved dating of the Kula Quaternary volcanic field and numerical modelling of the Gediz River terrace staircase. *Glob. Planet. Chang.* **2006**, *51*, 131–171. [[CrossRef](#)]
38. Görür, N.; Oktay, F.Y.; Seymen, I.; Şengör, A.M.C. Paleotectonic evolution of the Tuzgölü basin complex, Central Turkey: Sedimentary record of a Neo-Tethyan closure. In *The Geological Evolution of the Eastern Mediterranean*; Dixon, J.E., Robertson, A.H.F., Eds.; Geol.Soc.London. Spec. Publ. No: London, UK, 1984; Volume 17, pp. 467–482.
39. Schildgen, T.; Cosentino, D.; Bookhagen, B.; Niedermann, S.; Yıldırım, C.; Echtler, H.; Wittman, H.; Strecker, M. Multi-phased uplift of the southern margin of the Central Anatolian plateau, Turkey: A record of tectonic and upper mantle processes. *Earth Planet. Sci. Lett.* **2012**, *317*, 85–95. [[CrossRef](#)]
40. Şengör, C.; Yılmaz, Y. Tethyan evolution of Turkey: A plate tectonic approach. *Tectonophysics* **1981**, *75*, 181–241. [[CrossRef](#)]
41. Atalay, İ. *Geomorphology and Soil Geography of the Muş Plain and Its Surrounding*; Ege University Press: İzmir, Turkey, 1983.
42. Şaroğlu, F.; Güner, Y. The factors which effect to the geomorphological development of the Eastern Anatolia: The relations between geomorphology, tectonism and volcanism. *TJK Bull.* **1981**, *24*, 39–50.
43. Miall, A. *The Geology of Fluvial Deposits*; Springer: Berlin/Heidelberg, Germany, 1996.
44. Murray, A.; Wintle, A. Luminescence dating of quartz using an improved single-aliquot regenerative-dose protocol. *Radiat. Meas.* **2000**, *32*, 57–73. [[CrossRef](#)]
45. Gülen, L.; Pınar, A.; Kalafat, D.; Özel, N.; Horasan, G.; Yılmaz, M.; Işıkar, A.M. Surface fault breaks, aftershock distribution, and rupture process of the 17 August 1999 İzmit, Turkey Earthquake. *Bull. Seismol. Soc. Am.* **2002**, *92*, 230–244. [[CrossRef](#)]
46. Vandenberghe, J. Changing fluvial processes under changing periglacial conditions. *Zeitschr. F.Gemorphol. Suppl. Bd.* **1993**, *88*, 17–28.
47. Vandenberghe, J. A typology of Pleistocene cold-based rivers. *Quat. Int.* **2001**, *79*, 111–121. [[CrossRef](#)]
48. Pickarski, N.; Kwiecien, O.; Langgut, D.; Litt, T. Abrupt climate and vegetation variability of eastern Anatolia during the last glacial. *Clim. Past* **2015**, *11*, 1491–1505. [[CrossRef](#)]
49. Messenger, E.; Belmecheri, S.; Von Grafenstein, U.; Nomade, S.; Ollivier, V.; Voinchet, P.; Puaud, S.; Courtin-Nomade, A.; Guillou, H.; Mgeladze, A.; et al. Late Quaternary record of the vegetation and catchment-related changes from Lake Paravani (Javakheti, South Caucasus). *Quat. Sci. Rev.* **2013**, *77*, 125–140. [[CrossRef](#)]
50. Şenkul, Ç.; Doğan, U. Vegetation and climate of Anatolia and adjacent regions during the Last Glacial period. *Quat. Int.* **2013**, *302*, 110–122. [[CrossRef](#)]